# Chapter 6

# fs-Dynamics of Small Gold Clusters: Results and Discussion

In the previous chapter, the reaction kinetics of small noble metal clusters towards oxygen ($O_2$) and carbon monoxide ($CO$) could be characterized and the derived catalytic cycle for the oxidation reaction of carbon monoxide ($CO$) to carbon dioxide ($CO_2$) on gas-phase $Au_2^-$ clusters was shown for the first time. In order to gain a better insight into the nuclear dynamics of the molecular systems involved in these reactions, femtosecond (fs) time-resolved spectroscopy is a powerful technique. As discussed in chapter 3, the negative-to-neutral-to-positive (NeNePo) spectroscopy allows the study of the nuclear dynamics of neutral molecular systems and presents the advantage of mass selection of the investigated systems prior to and after the interaction with the laser field. In this chapter, the results obtained from the investigations of the fs-dynamics of gold clusters *via* NeNePo spectroscopy will be presented. First, the fs-dynamics of pure gold clusters ($Au_2$, $Au_3$) will be studied. The influence of the initial temperature of the molecular ensemble on the nuclear dynamics of gold clusters will be discussed. Subsequently, the first steps in the development of a new spectroscopic method referred to as *reactive NeNePo*, employed for the investigation of the fs-dynamics of cluster-adsorbate systems, will be presented.

## 6.1 NeNePo Spectroscopy on $Au_2^-$ Clusters

In chapter 5, the reactivity of negatively charged gold dimers towards oxygen and carbon monoxide was presented. It could be shown that $Au_2^-$ clusters are able to catalyze the oxidation reaction of carbon monoxide. In order to fully understand this chemical process, it is important to investigate the nuclear dynamics of pure clusters and cluster-adsorbate complexes.

For this, the NeNePo spectroscopy was applied to the investigation of the fs-dynamics of gold dimers. After the production of the cluster beam and the alignment of the laser system, the data acquisition was performed as described in chapter 4. The NeNePo measurements on $Au_2^-$ clusters were carried out at an ion trap temperature of 100 $K$. The final goal of the experiments consists in the study of the fs-dynamics of cluster-adsorbate complexes *via* reactive NeNePo method (as will be shown in section 6.3). Since the reaction rate constants for the reactivity of negatively charged $Au_2^-$ clusters towards oxygen and carbon monoxide have a high value for a reaction temperature of 100 $K$, *i.e.* the concentration of the reaction products presents a maximum under the experimental conditions for the measurements presented here, this value was set as the initial temperature of the anionic gold dimers.

For the detachment process a wavelength of 323 $nm$ (3.84 $eV$) was chosen, while a wavelength of 410 $nm$ (3.03 $eV$) was employed for the ionization process. The vertical detachment energy ($VDE$) of the $Au_2^-$ clusters and the ionization potential ($IP$) of the neutral gold dimers were experimentally found to be $E_{VDE}(Au_2^-) = 2.01 \pm 0.01$ $eV$[138,158] and $E_{IP}(Au_2) = 9.20 \pm 0.21$ $eV$,[164] respectively. Since the ionization potential of the neutral gold dimers has a high value, which is experimentally difficult to obtain through a one-photon process, a multi-photon process will be involved in the probe step of the NeNePo measurements on negatively charged gold dimers. In order to provide sufficient energy for the multi-photon ionization process and to achieve a one-photon detachment process, the laser power of the pump and probe beams were chosen to be $P_{\lambda=323nm} = 1.5$ $mW$ and $P_{\lambda=410nm} = 10$ $mW$ at a repetition rate of 1 $KHz$, respectively.

Fig. 6.1 (a) and (b) show the NeNePo spectra for the $Au_2^-$ clusters measured under the experimental conditions discussed above. The positive $Au_2^+$ ion signal was recorded as a function of the delay time ($t_d$) between the pump and the probe pulse.

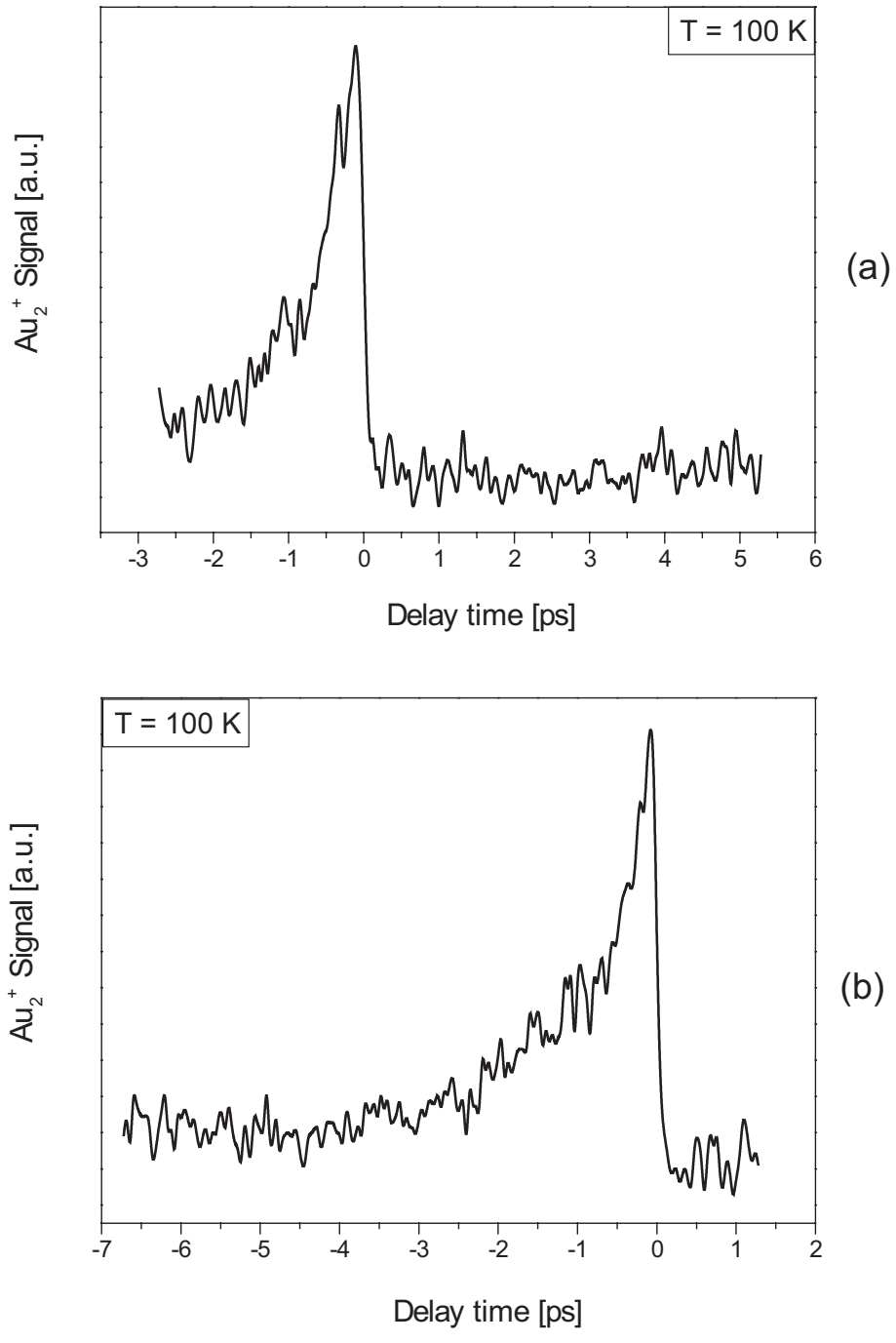


Figure 6.1: NeNePo spectra for $Au_2^-$ clusters measured at a temperature of 100 $K$. (a) and (b): the signal of the $Au_2^+$ clusters is depicted as a function of the delay time between the pump and the probe laser pulses. The parameters of the laser pulses are: $\lambda_{Pump} = 323\ nm$, $\lambda_{Probe} = 410\ nm$, $P_{Pump} = 1.5\ mW$, $P_{Probe} = 10\ mW$. For negative values of the delay time the pump and the probe pulse are reversed ($\lambda_{Pump} = 410\ nm$, $\lambda_{Probe} = 323\ nm$).

For positive values of the delay time ($t_d > 0$), the ultraviolet laser beam represents the pump pulse and the blue laser beam represents the probe pulse. For negative values of the delay time ($t_d < 0$), the order of the pump and the probe is reversed and, in this case, the blue laser beam represents the pump pulse, while the ultraviolet laser beam represents the probe pulse.

From Fig. 6.1 (a), it can be seen that for positive delay times ($\lambda_{Pump} = 323\ nm$, $\lambda_{Probe} = 410\ nm$, $P_{Pump} = 1.5\ mW$, $P_{Probe} = 10\ mW$) no transient signal can be identified. Surprisingly, for negative delay times ($\lambda_{Pump} = 410$ nm, $\lambda_{Probe} = 323$ nm, $P_{Pump} = 10$ mW, $P_{Probe} = 1.5$ mW) the measured signal shows a significant time-dependent behavior (see Fig. 6.1 (b)). Starting from $t_d = 0\ fs$ delay time, the signal increases abruptly and decreases exponentially to the value measured for $t_d > 0$. It is important to note that no $Au^+$ fragment was detected for any investigated experimental conditions. For the interpretation of the measured pump-probe spectra, information about the potential energy curves of the anionic, neutral and cationic gold dimers are required.

In the following, a short overview of the experimentally observed and theoretically calculated spectroscopic constants for the gold dimers will be presented. The ground state of the negatively charged $Au_2^-$ clusters ($X\ ^2\Sigma_u^+$) was investigated by Ho *et al.*, *via* high resolution photoelectron spectroscopy.[138] The authors found an equilibrium bond length of $r_e = 2.58\ \mathring{A}$, a dissociation energy of $D_e = 1.92\ eV = 15485.7\ cm^{-1}$ and a vibrational frequency of $\omega_e = 149\ cm^{-1}$.[138] Theoretical *ab initio* calculations of the electronic ground state of the $Au_2^-$ clusters predict a bond length of $r_e = 2.64\ \mathring{A}$, a dissociation energy of $D_e = 2.01\ eV = 16211.6\ cm^{-1}$ and a vibrational frequency of $\omega_e = 134.5\ cm^{-1}$.[157] The electronic ground state of positively charged $Au_2^+$ clusters ($X\ ^2\Sigma_g^+$) was investigated by combined ion mobility measurements and density functional calculations. From these studies, a bond length of $r_e = 2.62\ \mathring{A}$ and a dissociation energy of the $Au_2^+$ clusters of $D_e = 2.32\ eV = 18711.9\ cm^{-1}$ was obtained.[125] The vibrational frequency of the electronic ground state of the cationic gold dimers was theoretically calculated to be $\omega_e = 177\ cm^{-1}$.[165]

The neutral gold dimers $Au_2$ were intensively studied, experimentally and theoretically. Photoelectron spectroscopy, two-photon ionization spectroscopy as well as optical absorption spectroscopy were employed for the detection and characterization of the electronic ground and excited states of the neutral gold dimers in the

gas-phase.[132,138,158,164,166] Neutral gold dimers embedded in matrices were studied as well by using different spectroscopic methods.[167–169] Theoretical investigations based on relativistic methods were carried out, in order to assign the spectroscopic features of neutral gold dimers.[157,161,170–172]

The ground state ($X\ ^1\Sigma_g^+$) of the neutral gold dimers $Au_2$ was investigated by means of photoelectron spectroscopy and a frequency $\omega_e = 190.9\ cm^{-1}$, an equilibrium bond length $r_e = 2.47\ \mathring{A}$ and a dissociation energy $D_e = 2.29\ eV = 18469.9\ cm^{-1}$ were found.[138] Theoretical calculations predict for the electronic ground state $X\ ^1\Sigma_g^+$ of the $Au_2$ clusters a bond length $r_e = 2.45\ \mathring{A}$,[165] a vibrational frequency $\omega_e = 193\ cm^{-1}$,[161] and a dissociation energy $D_e = 2.28\ eV = 18389.3\ cm^{-1}$.[157] The first excited state of the neutral gold dimers is a triplet state denoted as $a^3\Sigma_u^+$ and corresponds to an excitation of one of the $6s$ electrons from a $\sigma_g$ orbital into an antibonding $\sigma_u^*$ orbital. From resonant two-photon ionization spectroscopy experiments on jet-cooled $Au_2$ clusters, Bishea *et al.* obtained a frequency of $\omega_e = 87.8\ cm^{-1}$ and a dissociation energy of $D_e = 0.23\ eV = 1840\ cm^{-1}$.[164] Due to the small dissociation energy, the authors consider the $a^3\Sigma_u^+$ state as an extremely weak bound state.[164] Itkin *et al.* calculated the spectroscopic constants of the electronic ground and excited states of $Au_2$ neutral clusters and found an equilibrium bond length of $r_e = 2.74\ \mathring{A}$ for the first excited state $a^3\Sigma_u^+$.[172]

As discussed in chapter 5, one of the consequences of the relativistic effects in gold is the strong spin-orbit coupling, which leads to a mixing of the electronic states. For the neutral gold dimers, the ground and the first excited state can be described in a good approximation according to case (a) of Hund's rules[173] and can be considered as pure states. All higher excited states require a description according to case (c) of Hund's rules[173] for mixed states, which makes the assignment and interpretation of these states more complicated.

The second excited state of the neutral gold dimers, which was observed in gas-phase experiments is the $A'\ 1_u$ state.[158,164] The spectroscopic constants for this state are: $r_e = 2.55\ \mathring{A}$,[174] $\omega_e = 223.6\ cm^{-1}$ and $D_e = 1.18\ eV = 9500.7\ cm^{-1}$.[164] The next energetically higher lying excited state of the gold dimers is denoted as $A\ 0_u^+$ and presents an equilibrium bond length of $r_e = 2.57\ \mathring{A}$, a vibrational frequency of $\omega_e = 142.6\ cm^{-1}$ and a dissociation energy of $D_e = 0.99\ eV = 7987.2\ cm^{-1}$.[164] The $B'\ 1_u$ state represents the fourth excited state of the neutral gold dimers, which was

experimentally observed. This state is characterized by the following spectroscopic constants: $r_e = 2.57\ \mathring{A}$, $\omega_e = 126.8\ cm^{-1}$, and $D_e = 0.45\ eV = 3638.8\ cm^{-1}$.[164]

The highest excited state of the neutral gold dimers, that could be identified in gas-phase experiments is the $B\ 0_u^+$ state.[158,164] For this state, an equilibrium bond length of $r_e = 2.52\ \mathring{A}$, a vibrational frequency of $\omega_e = 179.9\ cm^{-1}$ and a dissociation energy of $D_e = 1.76\ eV = 14225.3\ cm^{-1}$ were obtained.[164] The high value of the dissociation energy is an indication of an extremely strong bound state compared to other excited states of neutral $Au_2$ clusters. Bishea *et al.* describe this excited state as an ion pair state ($Au^+ - Au^-$) of the neutral gold dimers.[164]

The experimentally measured and theoretically calculated spectroscopic constants for the anionic, neutral and cationic gold dimers are summarized in table 6.1.

| **State** | $\mathbf{r_e}$**[Å]** | $\omega_\mathbf{e}$**[cm$^{-1}$]** | $\mathbf{D_e}$**[eV]** | $\mathbf{\Delta_e}$**[eV]** |
|---|---|---|---|---|
| $Au_2^-$ - $X\ ^2\Sigma_u^+$ | 2.58[a] | 149[a] | 1.92[a] | -2.01[c,g] |
| $Au_2$ - $X\ ^1\Sigma_g^+$ | 2.47[a] | 190[a] | 2.29[a] | 0 |
| $a^3\Sigma_u^+$ | 2.74[b] | 87.8[c] | 0.23[c] | 2.01[g] |
| $A'\ 1_u$ | 2.55[d] | 223.6[c] | 1.18[c] | 2.24[g] |
| $A\ 0_u^+$ | 2.57[c] | 142.6[c] | 0.99[c] | 2.37[g] |
| $B'\ 1_u$ | 2.57[c] | 126.8[c] | 0.45[c] | 2.91[g] |
| $B\ 0_u^+$ | 2.52[c] | 179.9[c] | 1.76[c] | 3.14[g] |
| $Au_2^+$ - $X\ ^2\Sigma_g^+$ | 2.62[e] | 177[f] | 2.32[e] | 9.20[c] |

Table 6.1: The experimentally measured and theoretically calculated spectroscopic constants for the $Au_2^-/Au_2/Au_2^+$ clusters. [a] Ho *et al.*,[138] [b] Itkin *et al.*,[172] [c] Bishea *et al.*,[164] [d] James *et al.*,[174] [e] Gilb *et al.*,[125] [f] Barysz *et al.*,[165] [g] Handschuh *et al.*[158] $\Delta_e$ represents the energetic position of the respective states relative to the electronic ground state of the neutral gold dimer obtained from photoelectron spectroscopy measurements.

A diatomic molecule represents the most simple molecular system, since only one vibrational degree of freedom is available. In a good approximation, the potential

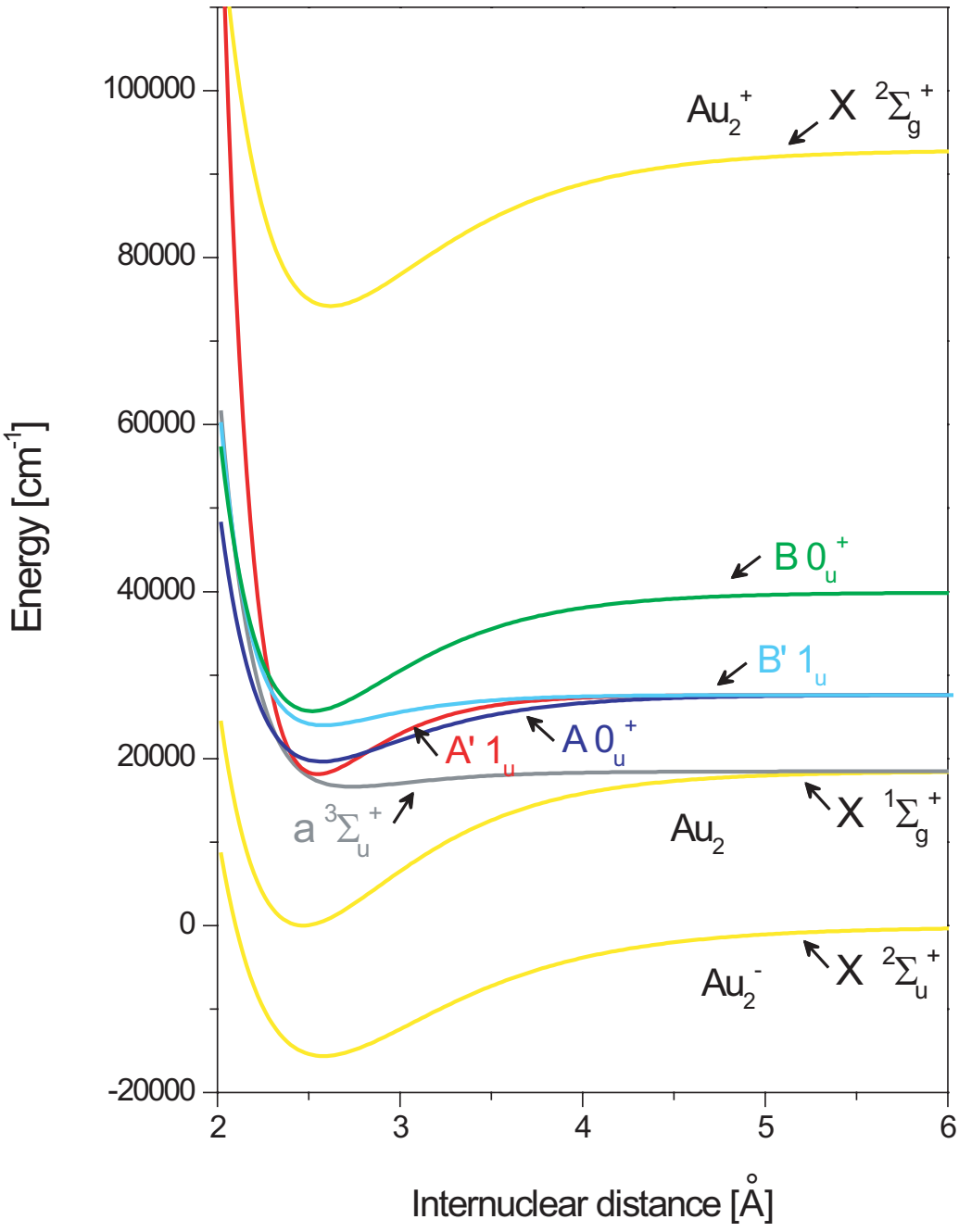


Figure 6.2: Morse-potential energy curves of the negative, neutral and positive gold dimers ($Au_2^-/Au_2/Au_2^+$) with all experimentally observed electronic excited states of the neutral $Au_2$ clusters.

energy curves can be described by using the Morse potential:[69]

$$V(R) = D_e[1 - e^{-a(R-R_e)}]^2 \tag{6.1}$$

where $D_e$ represents the dissociation energy of the molecule for a given electronic state, $R_e$ represents the equilibrium bond length for an electronic state of the molecule and $R$ represents the distance between the two nuclei. $a$ is a quantity which depends on the specific properties of the molecule and is given by the expression:

$$a = \left(\frac{m_r}{2D_e}\right)^{1/2} \omega_e \tag{6.2}$$

where $m_r$ denotes the reduced mass of the molecule and $\omega_e$ denotes the vibrational frequency of the molecule for a given electronic state. By inserting the experimental values found in literature for $D_e$, $R_e$ and $\omega_e$, which are summarized in table 6.1, into the expressions 6.1 and 6.2, the Morse potential energy curves for the negative ($Au_2^- - X\ ^2\Sigma_u^+$), neutral ($Au_2 - X\ ^1\Sigma_g^+$) and positive ($Au_2^+ - X\ ^2\Sigma_g^+$) gold dimers, including the electronic excited states of the neutral ($a\ ^3\Sigma_u^+$, $A'\ 1_u$, $A\ 0_u^+$, $B'\ 1_u$, $B\ 0_u^+$), can be calculated. The results are presented in Fig. 6.2, where the potential energy curves for the $Au_2$ clusters are depicted as a function of the internuclear distance. With the help of this potential energy curve scheme, the interpretation of the measured NeNePo spectra presented in Fig. 6.1 (a) and (b) can be performed.

In the following, the discussion will focus on the experimental results obtained for positive values of the delay time ($t_d > 0$) between the pump and the probe laser pulses. Fig. 6.1 (a) shows a NeNePo spectrum measured up to $t_d = 6\ ps$ delay time. From this spectrum, it can be seen that for positive values of the delay time no time-dependent dynamics can be observed. Fig. 6.3 shows the scheme of the pump-probe process for positive values of the delay time, where the ultraviolet laser pulse ($\lambda_{Pump} = 323\ nm$, $P_{Pump} = 1.5\ mW$) represents the pump and the blue laser pulse ($\lambda_{Probe} = 410\ nm$, $P_{Probe} = 10\ mW$) represents the probe. By comparing the energy of the pump pulse ($3.84\ eV$) to the vertical detachment energy of the $Au_2^-$ clusters ($E_{VDE}(Au_2^-) = 2.01\ eV$[138,158]) and the energetic position of the first excited state $a\ ^3\Sigma_u^+$ of the neutral gold dimers, which is situated about $4\ eV$ above the anionic ground state,[158,163] it can be deduced that only the ground state $X\ ^1\Sigma_g^+$ of the neutral gold dimers $Au_2$ can be populated through a one-photon detachment process. From photoelectron spectra measured on $Au_2^-$ clusters it was observed that

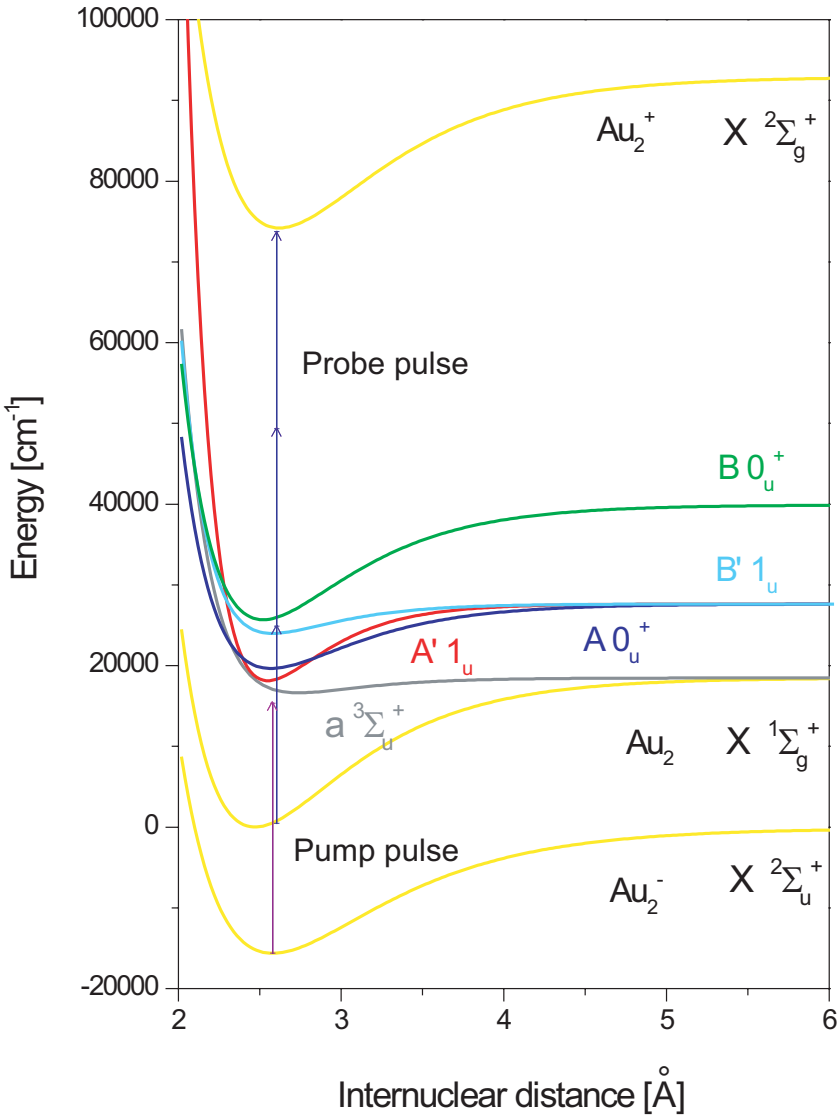


Figure 6.3: The pump-probe scheme for the NeNePo measurements on $Au_2^-$ clusters corresponding to positive values of the delay time between the pump and the probe laser pulses ($t_d > 0$). The vertical arrows represent the pump and the probe laser pulses. The characteristics of the laser pulses are: $\lambda_{Pump} = 323\ nm$, $P_{Pump} = 1.5\ mW$, $\lambda_{Probe} = 410\ nm$, $P_{Probe} = 10\ mW$.

only low vibrational levels of the neutral gold dimers present favorable Franck-Condon factors (up to $\nu(Au_2) = 7$) and therefore, only these vibrational levels are populated through a photodetachment process.[138] Thus, the fs-pump pulse creates a wave packet

on the ground state of the neutral cluster. The wave packet starts to evolve on the respective potential energy curve and after a given delay time the second laser pulse probes the dynamics of the wave packet.

When the pump pulse populates the ground state of the gold dimers, one would expect to see the oscillations of the wave packet, as previously observed in the case of the NeNePo experiments on $Ag_2^-$ clusters performed in the group of Prof. L. Wöste, where an oscillation with a frequency of $f = 185\ cm^{-1}$ was identified. This corresponds to the vibrational frequency of the neutral silver dimer in its electronic ground state.[79] Since no wave packet dynamics can be observed for positive values of the delay time, it can be assumed that the energy of the probe pulse is not sufficient to ionize the ground state of the gold dimer ($E_{IP}(Au_2) = 9.20\ \pm\ 0.21\ eV$[164]). The ionization process is considered to be a three-photon process ($3\times\ 3.03\ eV = 9.09\ eV$), as shown in Fig. 6.3. An ionization step which involves four blue photons would lead to a direct transition anion $\rightarrow$ cation and to the disappearance of any time-dependent signal for positive as well as for negative values of the delay time. In conclusion, the lack of wave packet dynamics in the transient signal for positive delay times ($t_d > 0$) can be rationalized as a consequence of the high ionization energy for gold dimers.

In the following, the experimental results obtained for negative values of the delay time between the pump and the probe pulses ($t_d < 0$) will be discussed. Fig. 6.4 shows the pump-probe scheme corresponding to negative delay times, when the blue laser pulse represents the pump pulse ($\lambda_{Pump} = 410\ nm$, $P_{Pump} = 10\ mW$) and the ultraviolet laser pulse represents the probe pulse ($\lambda_{Probe} = 323\ nm$, $P_{Probe} = 1.5\ mW$). As shown in Fig. 6.1 (b), for negative delay times ($t_d < 0$) an exponential decay of the NeNePo signal is observed. By fitting the experimental data and taking into account the temporal width of the laser pulses, a decay time of $\tau = 1.35\ \pm\ 0.24\ ps$ is obtained. Considering that three blue photons are involved in the photodetachment process ($3\times\ 3.03 = 9.09\ eV$), a wave packet is created on an highly excited electronic state of the neutral gold dimers after the detachment process. By calculating the difference between the energy of the pump pulse ($E(Pump\ pulse) = 9.09\ eV$) and the vertical detachment energy of the $Au_2^-$ clusters ($E_{VDE}(Au_2^-) = 2.01\ eV$[138,158]), a value of $7.08\ eV = 57103.6\ cm^{-1}$ above the electronic ground state of the neutral $Au_2$ clusters is obtained for the energetic position of the excited state. The evolution of the wave packet on this highly excited state is interrogated by the probe pulse. As

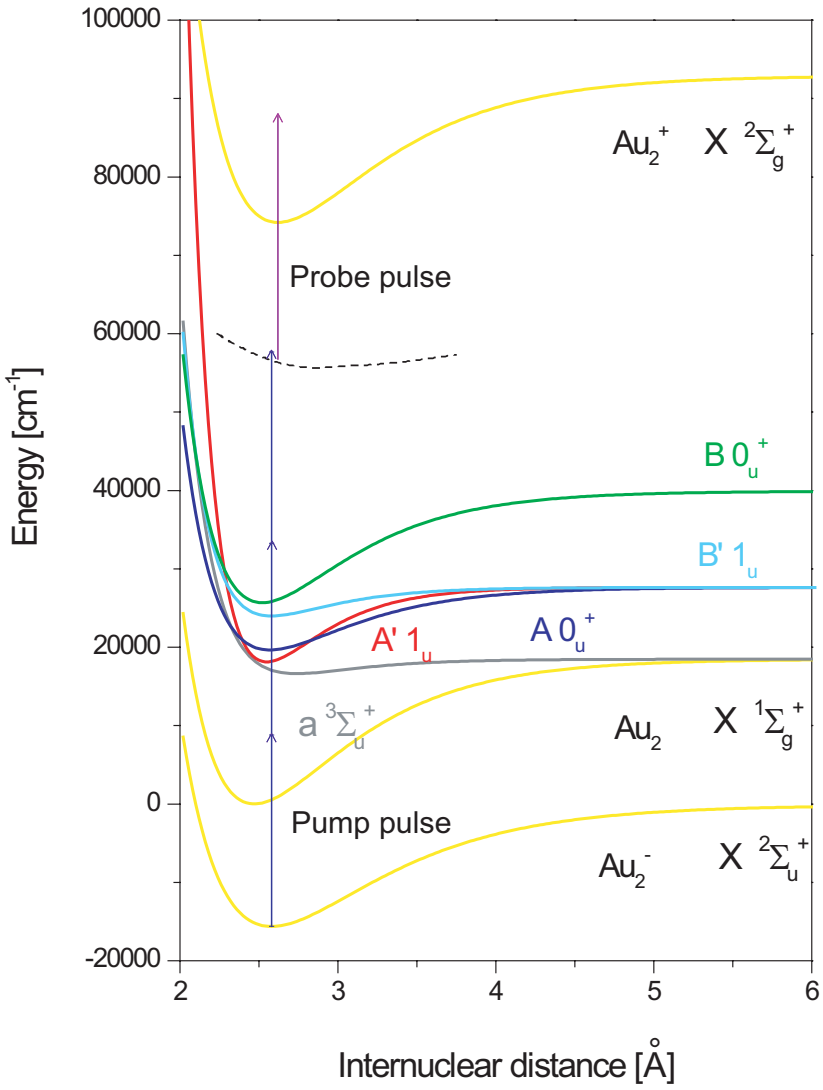


Figure 6.4: The pump-probe scheme for the NeNePo measurements on $Au_2^-$ clusters corresponding to negative values of the delay time between the pump and the probe laser pulses ($t_d < 0$). The vertical arrows represent the pump and the probe laser pulses. The characteristics of the laser pulses are: $\lambda_{Pump} = 410\ nm$, $P_{Pump} = 10\ mW$, $\lambda_{Probe} = 323\ nm$, $P_{Probe} = 1.5\ mW$. The dashed line represents the experimentally observed high excited state of the neutral gold dimers .

discussed above, the probe process involves one ultraviolet photon ($1 \times\ 3.84\ eV$), due to the low intensity of the ultraviolet laser beam.

The highest excited states which were experimentally observed in spectroscopic

measurements on matrix-isolated $Au_2$ clusters are situated at 6.26 $eV$ = 50505 $cm^{-1}$ and 5.96 $eV$ = 48076 $cm^{-1}$ above the ground state of the neutral dimer and these states are currently not assigned.[166–169] Due to the lack of theoretical calculations, the exponential decay of the observed excited state can not be unambiguously assigned. Therefore, the possible processes which could lead to the observed decay of the experimentally measured $Au_2^+$ signal will be outlined. One possible interpretation of the experimental data is based on a dissociation process. If the observed excited state has a dissociative or a predissociative character, the neutral excited gold dimer will fragmentate. This could lead to an exponential decay of the population in the favorable Franck-Condon region for the ionization process. Another process which could be involved is a radiationless transition into another electronic state. A radiationless transition occurs at the crossing point of two potential energy curves and the time scale for this type of processes is on the order of $10^{-10}s - 10^{-13}s$.[69] Since the measured excited state lies about 7 $eV$ above the ground state of the neutral, it could be possible that a crossing point with another electronic state is present. In this case, the measured decay time would characterize the coupling between two excited electronic states of the gold dimer.

In conclusion, a previously unidentified excited state of the neutral gold dimer which is located about 7 $eV$ above the ground state is observed for the first time. A decay time of $\tau = 1.35 \pm 0.24$ $ps$ is measured, which could be due to a dissociation process of the neutral $Au_2$ clusters or a radiationless transition into another electronic state. However, theoretical calculations are required in order to elucidate the character of the experimentally observed high excited state of the neutral $Au_2$ clusters.

## 6.2 NeNePo Spectroscopy on $Au_3^-$ Clusters

After the investigation of $Au_2$ clusters, the study of the fs-dynamics of $Au_3$ clusters was performed *via* NeNePo spectroscopy. The experiments were carried out as described in chapter 5. Fig. 6.5 (a) and (b) show the NeNePo measurements performed on negatively charged gold trimers measured at an ion trap temperature of $T_{octopole} = 20$ $K$. The signal of $Au_3^+$ clusters (Fig. 6.5 (a)) and $Au_2^+$-fragment clusters (Fig. 6.5 (b)) obtained through the NeNePo process was recorded as a function of

the delay time ($t_d$) between the pump and the probe laser pulses. The signal of $Au_2^+$ clusters arises from the fragmentation of the gold trimers. The measured NeNePo spectra shown in Fig. 6.5 are normalized to the maximum value of the $Au_3^+$ signal (peak B in Fig. 6.5 (a)). The pump and the probe laser pulses have a wavelength of $\lambda_{Pump} = 318\ nm$ ($3.90\ eV$), $\lambda_{Probe} = 414\ nm$ ($3.00\ eV$) and a power of $P_{Pump} = 2\ mW$, $P_{Probe} = 10\ mW$, respectively. The vertical detachment energy (VDE) and the ionization potential (IP) of the gold trimers have a value of $E_{VDE}(Au_3^-) = 3.9\ eV$[158,163] and $E_{IP}(Au_3) = 7.5\ eV$,[162] respectively. The power of the laser pulses was chosen so that the photodetachment process involves one ultraviolet photon ($1 \times\ 3.90\ eV$), while the ionization process of $Au_3$ clusters involves three blue photons ($3 \times\ 3.00\ eV$).

From Fig. 6.5 (a), it can be clearly seen that the NeNePo spectrum of $Au_3$ clusters exhibits a pronounced time-dependent behavior for positive values of the delay time between the pump and the probe laser pulses. Moreover, distinct features which are denoted with $A$, $B$, $C$, $D$ and $E$ (see Fig. 6.5 (a)) can be observed in the spectrum. Starting from $t_d = 0\ fs$ delay time, the $Au_3^+$ signal increases and, at approximately $t_d = 0.14\ ps$ peak $A$ appears. The maximum of the transient signal is observed for a value of the delay time of about $t_d = 0.32\ ps$ (peak $B$). On the descending part of the $Au_3^+$ signal, three features ($C$, $D$ and $E$) can be identified at $t_d = 0.65\ ps$ (peak $C$), $t_d = 1.04\ ps$ (peak $D$) and $t_d = 1.40\ ps$ (peak $E$). The features $B$, $C$, $D$ and $E$ show a regular temporal spacing, with a time interval between the peaks of approximately $t = 360\ \pm\ 30\ fs$, which represents a frequency of about $\omega = 93\ \pm\ 8\ cm^{-1}$.

In Fig. 6.5 (b), the transient signal of the $Au_2^+$-fragment clusters is presented as a function of the delay time between the pump and the probe pulses. By comparing the intensity of the NeNePo signal for $Au_3^+$ clusters (Fig. 6.5 (a)) to the $Au_2^+$-fragment cluster signal (Fig. 6.5 (b)), it can be observed that the intensity of the $Au_3^+$ signal is about one order of magnitude higher than the $Au_2^+$-fragment signal. The shape of the $Au_2^+$-fragment signal reflects all the features (denoted with $A$, $B$, $C$, $D$, and $E$) which are identified in the case of the $Au_3^+$ clusters. Taking into account that the ionization potential of the neutral gold dimers has a value of $E_{IP}(Au_2) = 9.20\ eV$,[164] four blue photons would be necessary to ionize the $Au_2$ clusters. Since the power of the probe laser beam was chosen in order to achieve a three-photon ionization process of gold trimers ($3 \times\ 3.00\ eV = 9.00\ eV$), it is most probable that the energy of the probe pulse is not sufficient for the ionization of the gold dimers produced by the

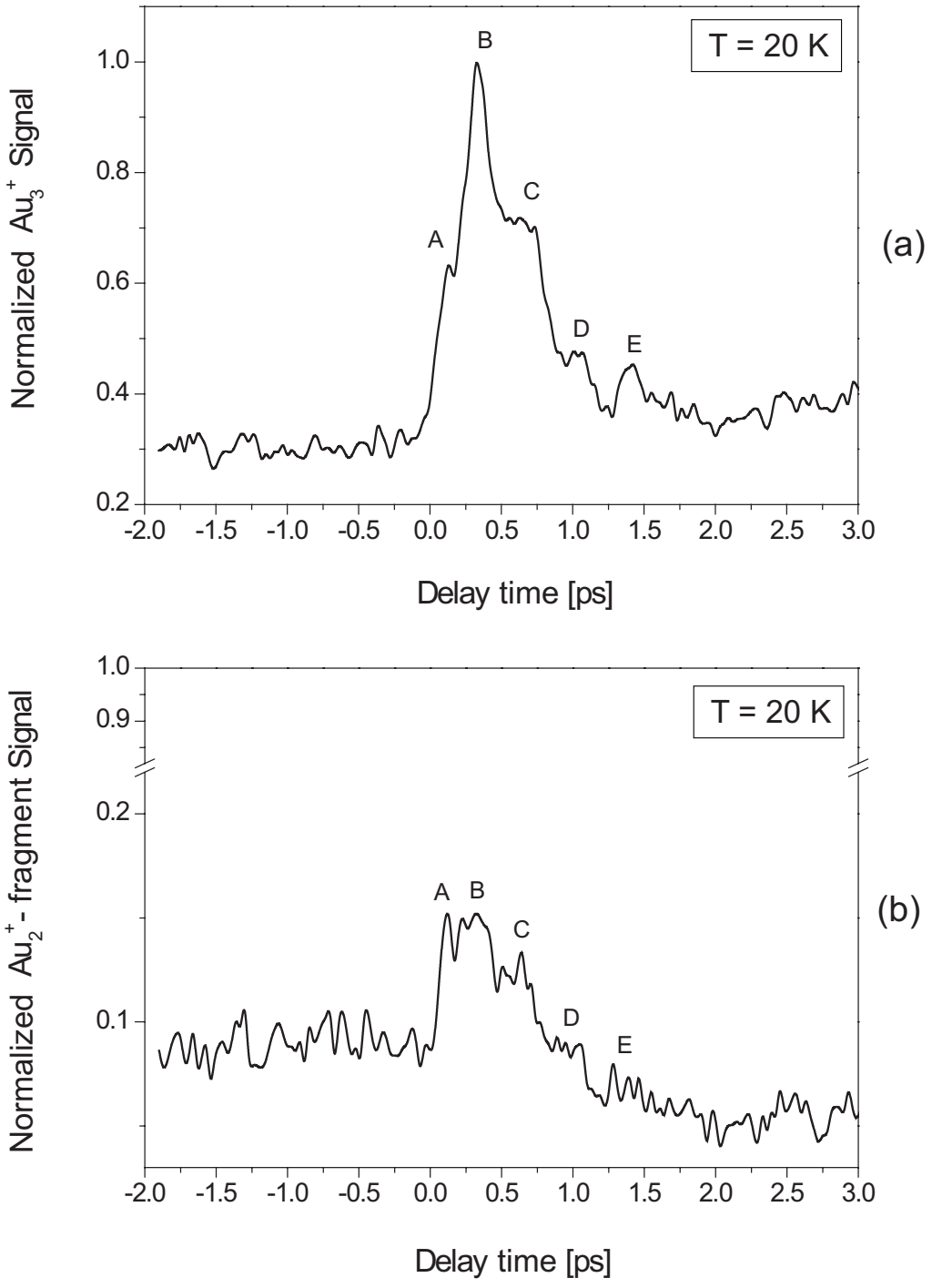


Figure 6.5: (a) The NeNePo spectrum of $Au_3$ clusters. The $Au_3^+$ signal is measured as a function of the delay time between the pump and the probe laser pulses. (b) The NeNePo spectrum of $Au_2^+$-fragment clusters. The measured spectra are normalized to the maximum of the $Au_3^+$ signal (peak $B$). The experimental parameters are: $\lambda_{Pump} = 318\ nm$, $\lambda_{Probe} = 414\ nm$, $P_{Pump} = 2\ mW$, $P_{Probe} = 10\ mW$ and $T_{octopole} = 20\ K$.

fragmentation of the neutral $Au_3$ clusters. Therefore, the fragmentation process does not occur on the neutral potential energy surface of the triatomic gold clusters and the $Au_2^+$-fragment signal arises from the fragmentation of the cationic gold trimers $Au_3^+$. Since no theoretical simulations of the NeNePo pump-probe signal for $Au_3$ clusters are available, a qualitative interpretation of the measured spectra will be performed, by comparing the presented results with data found in literature.

For the ground state of the negatively charged gold trimers a linear structure with a $D_{\infty h}$ symmetry and a bond length of about $r_e = 2.59$ Å was found by ion mobility measurements combined with theoretical calculations.[149,161,163] In the case of the $Au_3^+$ cations, experimental and theoretical investigation revealed that the most stable structure of the electronic ground state is a triangular structure with a $D_{3h}$ symmetry (equilateral triangle) and a bond length of $r_e = 2.64$ Å.[125,156,170]

Experimental studies on gas-phase neutral $Au_3$ clusters have been carried out by employing photoelectron spectroscopy and resonant two-photon ionization spectroscopy methods.[132,138,158,163,175] Optical absorbtion and emission spectra of gold trimers isolated in rare gas matrices have been measured as well.[167–169,176] From these studies, the energetic position of the electronic ground state, as well as a few excited states of the neutral $Au_3$ clusters were determined. However, there is no experimental information about the structure of the neutral gold trimers.

Due to the high complexity of the bonding in gold clusters, which exhibit strong relativistic effects, the theoretical modelling of the isomeric structures is a challenging task. Similar to the case of $Ag_3$ and $Cu_3$ neutral clusters, theoretical calculations of neutral gold trimers found a doubly degenerate $^2E'$ state with a $D_{3h}$ symmetry (equilateral triangle) for the electronic ground state. According to the Jahn-Teller theorem, this degeneracy is removed by splitting the $^2E'$ state in two states ($^2A_1$ and $^2B_2$).[138,161] Three isomeric structures were predicted for the neutral gold trimers: an acute isosceles triangle with a $C_{2v}$ symmetry corresponding to the $^2A_1$ state, an obtuse isosceles triangle ($C_{2v}$ symmetry) which corresponds to the $^2B_2$ state and a linear structure with a $D_{\infty h}$ symmetry which corresponds to the $^2\Sigma_u^+$ state.[157,161,170,177]

The results of the theoretical calculations found in literature are in contradiction with respect to the assignment of the most stable structure of the neutral gold trimers on the electronic ground state. Wesendrup *et al.* predicted the acute isosceles triangle ($^2A_1$) with a bond length of $r_e = 2.72$ Å and an apex angle of $\theta = 56.2°$ as the

most stable structure, while the obtuse isosceles triangle ($^2B_2$, $r_e = 2.61$ $\mathring{A}$, $\theta = 65.4°$) was found to be energetically approximately 0.007 $eV$ above the acute isosceles triangular structure.[170] The linear isomer ($^2\Sigma_u^+$, $r_e = 2.57$ $\mathring{A}$) was predicted to be a saddle point on the potential energy surface for the electronic ground state of the neutral $Au_3$ clusters and it was found to be situated approximately 0.1 $eV$ above the acute isosceles triangular structure. Moreover, the authors suggest that this linear structure of the neutral $Au_3$ clusters can be probed as "short-lived intermediate" in a NeNePo scheme experiment.[170] Balasubramanian *et al.* obtained the obtuse isosceles triangle $^2B_2$, having a bond length of $r_e = 2.60$ $\mathring{A}$ and an apex angle of $\theta = 65.7°$ as the absolute minimum of the potential energy surface for the electronic ground state of neutral $Au_3$ clusters.[177] The acute isosceles triangular structure $^2A_1$ with a calculated bond length of $r_e = 2.72$ $\mathring{A}$ and angle of $\theta = 56.4°$ lies 0.03 $eV$ higher. The linear isomeric structure ($r_e = 2.60$ $\mathring{A}$) is positioned about 0.48 $eV$ above the acute isosceles triangle.[177] However, both theoretical studies agree that the potential energy surface of the neutral gold trimer must be very shallow, since the energy difference between the two triangular isomers is predicted to be equal to or less than 0.03 $eV$. By considering the experimental and theoretical data found in literature, an interpretation of the experimental NeNePo spectra of $Au_3^-$ clusters will be given in the following.

The pump pulse ($\lambda_{Pump} = 318$ $nm$, $E_{Pump} = 3.9$ $eV$) neutralizes the negatively charged $Au_3^-$ clusters and, through the photodetachment process, a vibrational wave packet is created on the potential energy surface for the electronic ground state of the neutral gold trimer $Au_3$. Since the $Au_3^-$ anion has a linear structure, the initial configuration of the neutral $Au_3$ cluster will be linear according to the Franck-Condon principle. Similar to the case of NeNePo measurements performed on $Ag_3^-$ and $Ag_2Au^-$ clusters, at $t_d = 0$ $fs$ delay time the $Au_3^+$ signal is small (see Fig. 6.5 (a)). Theoretical simulations of the NeNePo signal carried out for $Ag_3$ and $Ag_2Au$ clusters showed that the linear isomers of the neutral clusters exhibit a higher ionization potential than the corresponding triangular isomers.[75,79] Therefore, the low value of the NeNePo signal at short delay times in the case of $Au_3$ clusters can be rationalized as a consequence of a high ionization potential of the neutral linear isomer.

Since the initial linear geometry of the neutral $Au_3$ clusters represents a non-equilibrium structure, the vibrationally excited gold trimer will undergo a geometrical

relaxation, *i.e.* it will start to bend from this linear geometry in order to reach the equilibrium triangular structure. A similar bending motion has been observed as well in the case of the NeNePo measurements performed on $Ag_3$ and $Ag_2Au$ clusters.[75,79] As the neutral gold trimer starts to bend, the wave packet created through the pump pulse starts to evolve on the potential energy surface of the neutral particle and enters the favorable Franck-Condon detection window for the ionization process. As a result, the $Au_3^+$ signal increases. During the evolution of the wave packet towards the first local minimum, the feature $A$ appears (see Fig. 6.5 (a)) in the NeNePo signal. The $Au_3^+$ transient signal reaches its maximum value at $t_d = 0.32\ ps$ (peak $B$ on Fig. 6.5 (a)). This peak can be correlated with a local minimum on the potential energy surface of the neutral gold trimers which corresponds to a bent structure. Since the NeNePo signal presents a high intensity, it seems that the Franck-Condon factors for the ionization process have a high value for this bent structure which is reached at $t_d = 0.32\ ps$ (peak $B$). Furthermore, theoretical calculations predict the existence of an excited state of the $Au_3$ clusters at an energy of about 3 $eV$ above the ground state.[177] The high intensity of peak $B$ might be attributed as well to a resonant three-photon ionization process, where the absorption of the first photon is resonant with this excited state.

If the bent geometry of the neutral gold trimer, which corresponds to peak $B$ would be the absolute minimum of the potential energy surface then the transient signal would remain constant at this maximum value. However, the $Au_3^+$ signal intensity decreases on a time scale of approximately $\tau = 1.4\ ps$ (see Fig. 6.5 (a)). This indicates that the structure of the neutral gold trimer which is probed at $t_d = 0.32\ ps$ delay time represents an intermediate geometry of the neutral gold trimer and the wave packet moves further towards the absolute minimum on the potential energy surface. Taking into account the theoretical calculations presented above, this bent intermediate structure could be attributed to the isosceles triangular isomer (acute, $^2A_1$ after Balasubramanian *et al.*[177] or obtuse, $^2B_2$ after Wesendrup *et al.*[170]).

Furthermore, oscillations of the $Au_3^+$ NeNePo signal which can be attributed to the oscillations of the wave packet on a time scale of $t = 360\ \pm\ 30\ fs$ are identified on the descending part of the $Au_3$ signal (peak $C$, $D$ and $E$ on Fig. 6.5 (a)). The time scale of the oscillations corresponds to a frequency of about $\omega = 93\ \pm\ 8\ cm^{-1}$. These oscillations superimposed on the transient signal decay suggest that a bifurcation

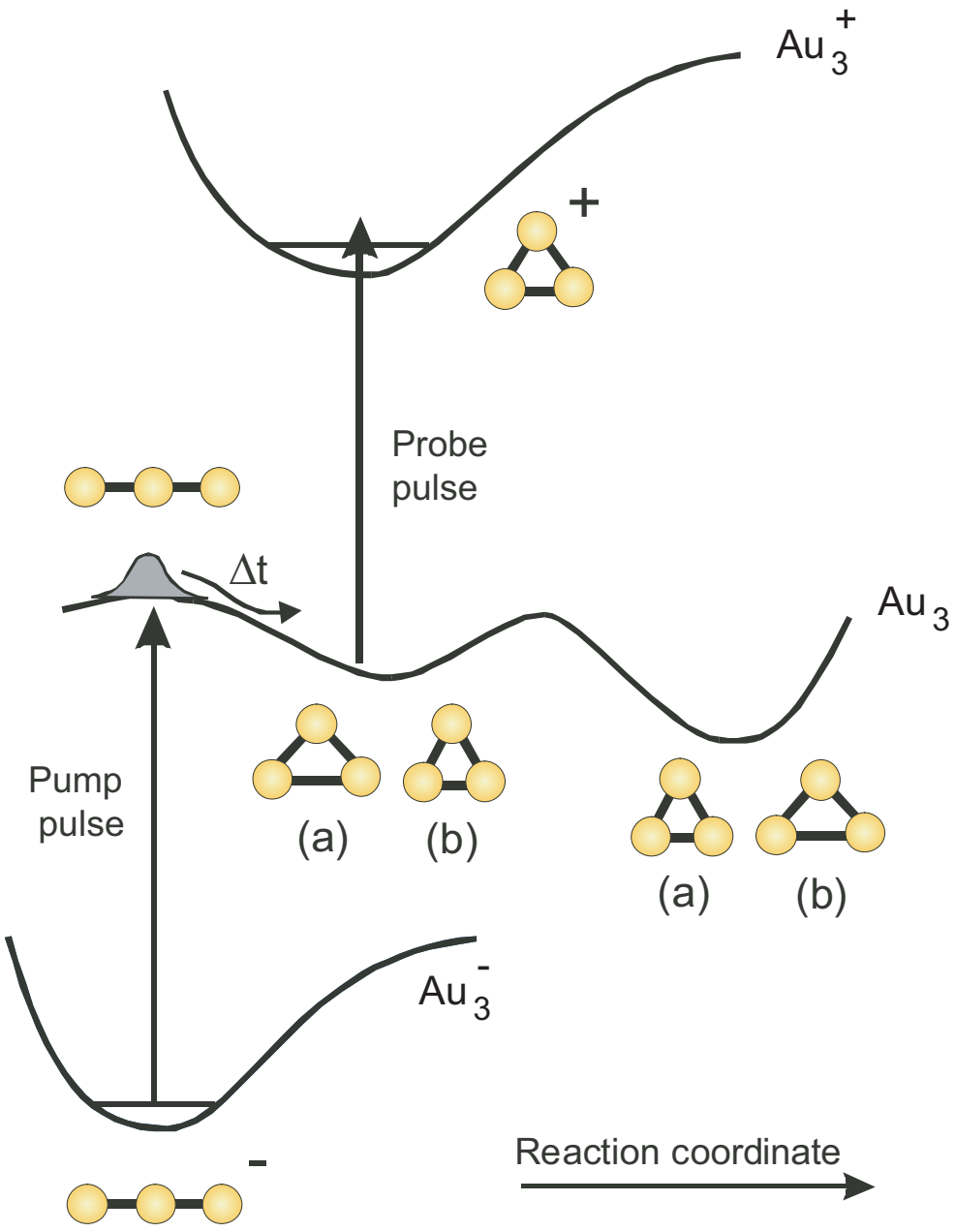


Figure 6.6: The NeNePo process for the case of $Au_3$ clusters in a schematic representation of the potential energy surfaces for anionic, neutral and cationic gold trimers. The theoretically calculated geometrical isomers of the neutral $Au_3$ clusters according to (a) Wesendrup *et al.*[170] and (b) Balasubramanian *et al.*[177] are depicted on the figure. The vertical arrows represent the pump and the probe pulse.

of the wave packet occurs. This means that the wave packet oscillates in the first local minimum (peak $B$) and, with every oscillation, part of the wave packet leaks to another state which might be assigned to the equilibrium geometry on the potential energy surface (obtuse isosceles triangular geometry according to Balasubramanian *et al.*[177] or acute isosceles triangular geometry according to Wesendrup *et al.*[170]). It seems that the Franck-Condon detection window for the ionization process is sensitive only to the intermediate geometry that is reached at $t_d = 0.32\ ps$ delay time and not to the final equilibrium geometry of the neutral gold trimer (see Fig. 6.5 (a)). Thus, the decrease of the $Au_3^+$ transient signal can be correlated with the evolution of the wave packet towards the equilibrium structure. A schematic representation of the pump-probe process for the NeNePo measurements in the case of gold trimers is presented in Fig. 6.6.

The observed vibrational frequency of the intermediate structure could correspond to a normal mode of the gold trimer (most probably the bending mode which is primarily involved in the geometrical relaxation) or to a superposition of different normal modes. Theoretical calculations performed for $Ag_3$ and $Cu_3$ neutral clusters predict vibrational frequencies for the intermediate isosceles triangular geometry of metal trimers which are on the same order of magnitude as the one observed in the experiments presented in this work ($\omega_{Bend}(Ag_3) = 99\ cm^{-1}$, $\omega_{Bend}(Cu_3) = 151\ cm^{-1}$).[161] However, due to the lack of theoretical studies, the observed vibrational frequency of $93\ \pm\ 8\ cm^{-1}$ for neutral $Au_3$ clusters can not be unambiguously assigned.

In order to gain further insights into the fs-dynamics of the neutral $Au_3$ clusters, temperature-dependent NeNePo measurements were performed. In these measurements, the temperature of the octopole ion trap was varied between $T_{octopole} = 20\ K$ and $T_{octopole} = 300\ K$. The temperature-dependent NeNePo spectra of gold trimers are presented in Fig. 6.7, where the signal of the positively charged gold clusters $Au_3^+$ is depicted as a function of the delay time between the pump and the probe pulse.

The measured NeNePo spectra are normalized to the maximum value of the $Au_3^+$ signal (peak $B$) taken for a temperature of the ion trap of $T_{octopole} = 20\ K$ (Fig. 6.7 (a)). The wavelengths and the energies of the pump and the probe pulses were maintained constant ($\lambda_{Pump} = 318\ nm$, $\lambda_{Probe} = 414\ nm$, $P_{Pump} = 2\ mW$, $P_{Probe} = 10\ mW$). By comparing the NeNePo spectrum measured at $T_{octopole} = 20\ K$ ion trap temperature (Fig. 6.7 (a)) to the spectra measured at higher temperatures

(Fig. 6.7 (b), (c), (d)), it can be observed that the peak structure of the $Au_3^+$ signal vanishes gradually and at an ion trap temperature of $T_{octopole} = 300\ K$ no peak can be detected anymore in the transient signal. This drastic temperature effect, which leads to a total change in the shape of the measured NeNePo spectra can be observed only in the case of gold clusters. For silver clusters $Ag_3$[73] and mixed silver-gold clusters $Ag_2Au$,[79] the increase of the temperature is manifested by a shift in the position of the signal maximum towards shorter delay times and only a slight change in the shape of the transient signal is detected. Therefore, the temperature effect must be correlated to the intrinsic properties of the gold clusters.

The increase of the ion trap temperature leads to a modification of the temperature of the initial anionic molecular ensemble. At a temperature of $T_{octopole} = 300\ K$, more vibrational energy levels of $Au_3^-$ cluster can be occupied compared to the low-temperature case. Through the photodetachment process, the anionic ensemble is projected on the potential energy surface for the electronic ground state of the neutral $Au_3$ clusters. Due to the increasing temperature of the initial anionic molecular ensemble, the wave packet created on the potential energy surface of the neutral is less localized. Since the isomeric triangular geometries of the neutral gold cluster have a maximal energy difference comparable with the thermal energy corresponding to an ion temperature of 300 $K$ and the potential energy surface of the neutral $Au_3$ clusters is predicted to be very shallow,[170,177] the wave packet can not be trapped into a local minimum and therefore, the peak structure of the transient signal vanishes. This interpretation is supported as well by the theoretical simulations of Wesendrup *et al.*, which predict that the neutral $Au_3$ clusters will not present a defined structure at room temperature.[170]

The delocalization of the wave packet as a function of temperature was theoretically calculated for neutral silver clusters $Ag_3$, by employing molecular dynamics (MD) simulations.[77] Bunches of trajectories of neutral $Ag_3$ clusters on the electronic ground potential energy surface for different temperatures of the molecular ensemble were simulated. The potential energy surface was calculated in $Q_s$ and $Q_x$ coordinates, that represent the symmetric stretching mode and the bending mode of the neutral silver trimer (see section 3.2). From these simulations, it was observed that the bunch of trajectories is narrow at low temperatures (50 $K$), while at a temperature of 300 $K$ the trajectories are more delocalized.[77] These theoretical calculations sup-

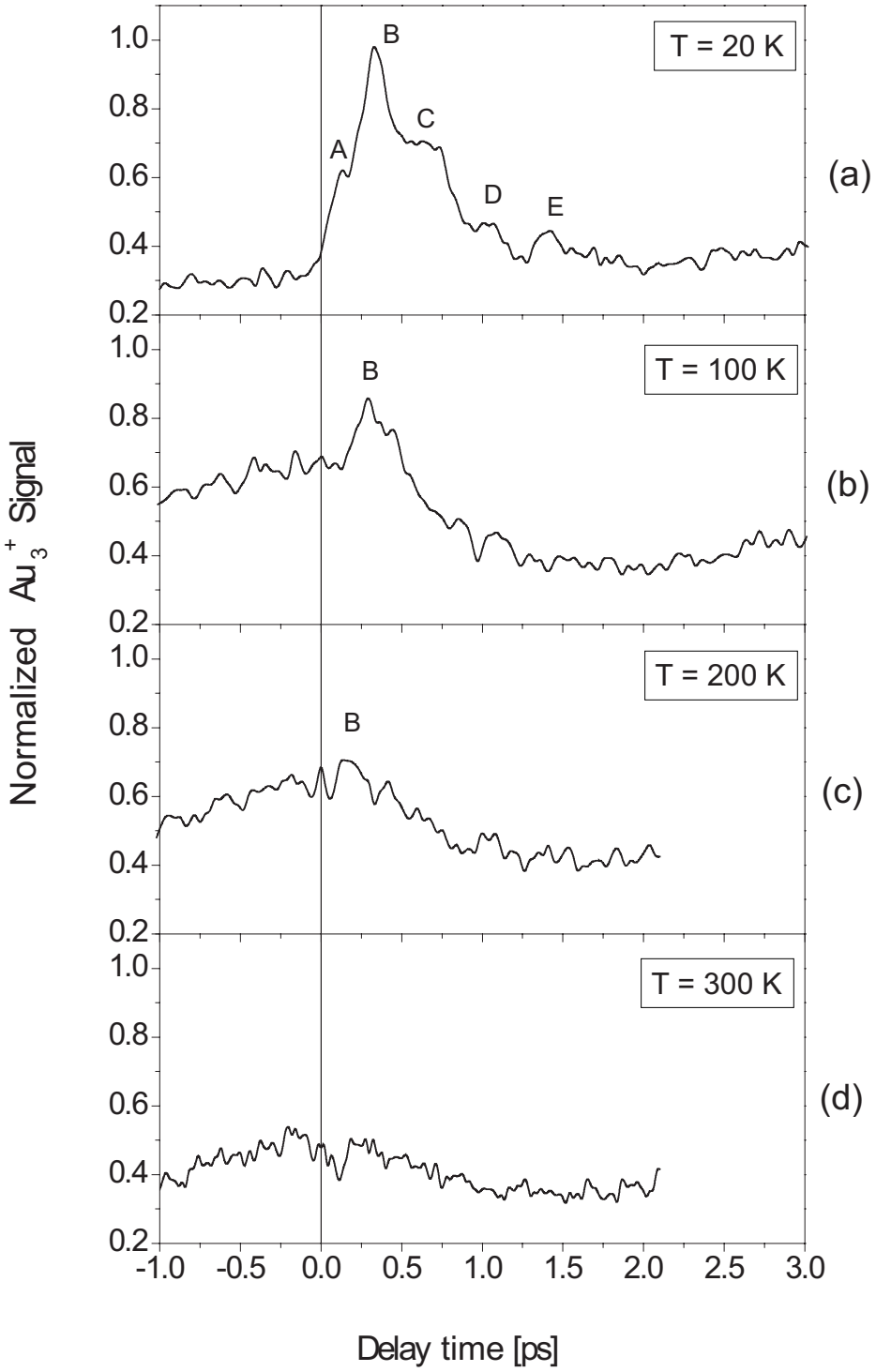


Figure 6.7: The NeNePo spectra of $Au_3$ clusters measured at different ion trap temperatures: (a) $T_{octopole} = 20\ K$, (b) $T_{octopole} = 100\ K$, (c) $T_{octopole} = 200\ K$ and (d) $T_{octopole} = 300\ K$. The $Au_3^+$ signal is measured as a function of the delay time between the pump and the probe laser pulses. The measured spectra are normalized to the maximum value of the $Au_3^+$ signal (peak $B$) measured at $T_{octopole} = 20\ K$. The experimental parameters are: $\lambda_{Pump} = 318\ nm$, $\lambda_{Probe} = 414\ nm$, $P_{Pump} = 2\ mW$, $P_{Probe} = 10\ mW$.

port the interpretation of the experimental NeNePo spectra of $Au_3$ clusters measured at different temperatures of the octopole ion trap.

In conclusion, the investigation of the fs-dynamics of the neutral $Au_3$ clusters is performed for the first time by using the NeNePo method. The $Au_3$ clusters show complicated nuclear dynamics. At low temperatures ($T_{octopole} = 20\ K$), the relaxation from the linear to an intermediate triangular geometry is observed. Moreover, oscillations of about $t = 360\ fs$ which correspond to a frequency of $\omega = 93\ cm^{-1}$ of the intermediate triangular structure can be identified in the NeNePo spectra. With increasing temperature, the peak structure of the transient signal vanishes and this result can be correlated with a delocalization of the wave packet on the potential energy surface for the electronic ground state of the neutral gold trimer. However, *ab initio* theoretical calculations of the potential energy surfaces of the anionic, neutral and cationic $Au_3$ clusters would be helpful for a detailed interpretation of the experimental data.

## 6.3 Reactive NeNePo Spectroscopy

One of the most important goals of the femtosecond time-resolved spectroscopy is the investigation of the sequential processes of a chemical reaction in real time, starting from educts and ending with the reaction products. The NeNePo spectroscopy allows for the study of the molecular fs-dynamics on the electronic ground state of a neutral system and presents the advantage of mass selection prior to and after the interaction with the laser field. Since most chemical reactions occur in neutral molecules, the NeNePo method is particularly suited for this purpose. For the study of the reaction educts (pure clusters), the "classical" NeNePo spectroscopy method can be successfully applied to the study of the fs-dynamics of gold dimers and trimers as it was shown in the previous sections (see section 6.1 and 6.2). In order to investigate the reaction products or reaction intermediates, that are usually cluster-adsorbate complexes, a new spectroscopic method was developed, which is referred to as *reactive NeNePo spectroscopy*. This method combines the methodology of the cluster reactivity measurements with the "classical" NeNePo femtosecond time-resolved experiments. The experimental realization is as following: first, negatively charged clusters are introduced in the octopole ion trap. There, the clusters interact with the

reactant gases for a given reaction time, until the desired reaction product (cluster-adsorbate complex) is formed. During the reaction product formation process, the laser beam is blocked by a mechanical shutter. When the yield of the reaction product to be investigated reaches a maximum, the shutter opens and the pump and the probe laser beams are directed inside the octopole ion trap and the cation signal is detected. It is important to note that in contrast to "classical" NeNePo spectroscopy where the detection of the positively charged clusters is performed continuously, the reactive NeNePo method requires a new ion trap cycle for every value of the delay time between the pump and the probe laser pulses. There are several possible scenarios relying on the principle of the reactive NeNePo spectroscopy, and three of them are depicted in Fig. 6.8:

- If the cluster-adsorbate complex is stable only as an anionic system, the cluster-adsorbate complex will dissociate after the photodetachment process and the dissociation products will be ionized with the probe laser pulse (see Fig. 6.8 (a)). In this case, information about the fs-dynamics of the cluster-adsorbate fragmentation process can be obtained.

- A chemical reaction which takes place on the neutral potential energy surface of a metal cluster can be started by photodetaching the excess electron of the negatively charged system with a first laser pulse. After the photodetachment process, the chemical reaction between the neutral system and reactant molecules takes place and the reaction products can be ionized and subsequently detected by using a second laser pulse, as shown in Fig. 6.8 (b). It is important to note that in this case, the time resolution of the experiment is limited by the reaction product formation rate, which is correlated to the collision frequency between the neutral clusters and the reactant molecules. In the experiments presented in this work, the lowest limit for the reaction product formation is on the millisecond time scale. Although this scenario is not a femtosecond pump-probe experiment which allows for the study of nuclear dynamics in real time, it presents the advantage of preparing a well defined neutral system through mass selection of the anions and a selective ionization of the reaction products and mass selection of the cations.

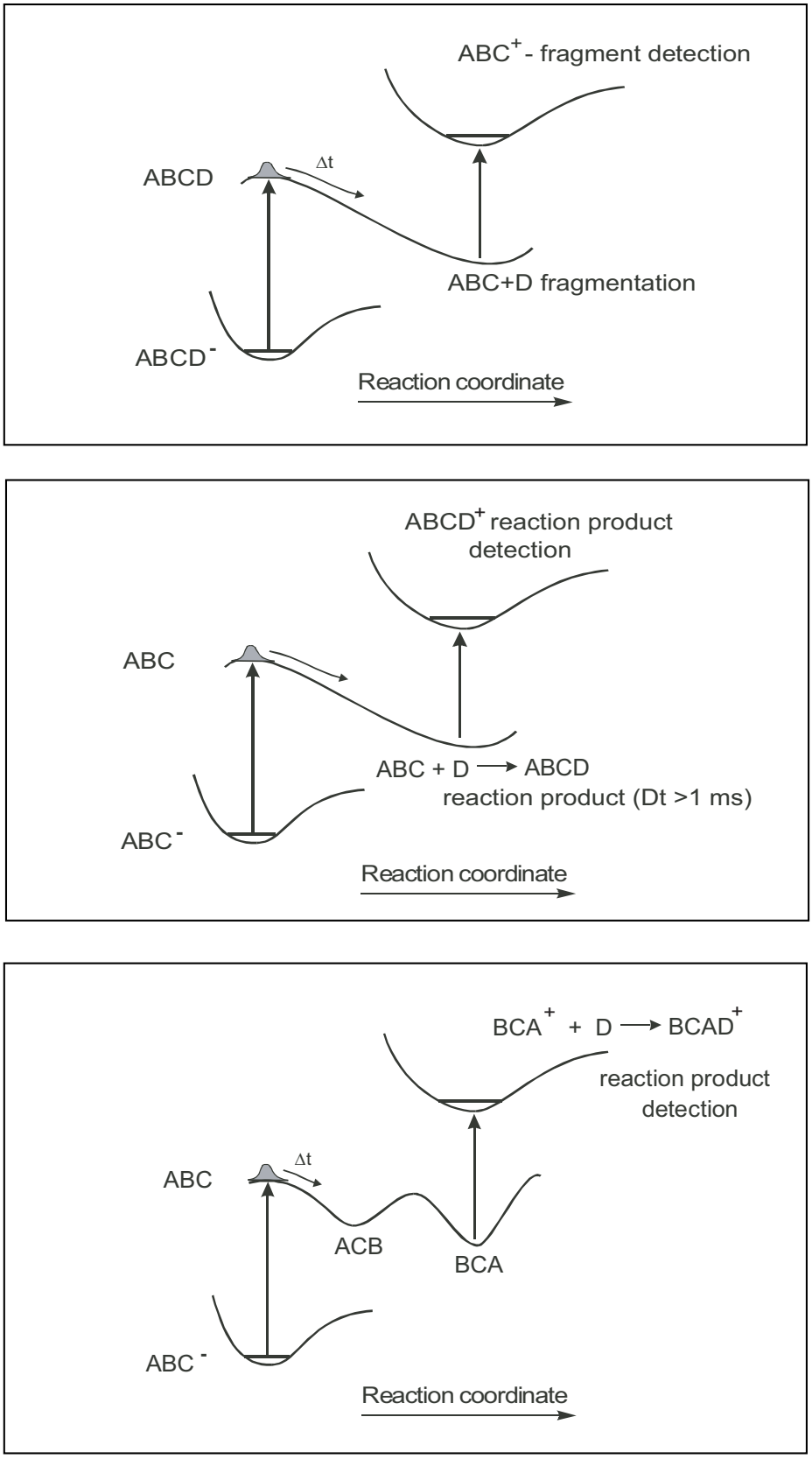


Figure 6.8: The schematic representation of several possible scenarios for reactive NeNePo spectroscopy. For details see text.

- Another possibility takes into account the isomerization process on the neutral and cationic potential energy surfaces when only one specific cationic isomer shows reactive properties. In this case, the pump laser pulse creates a neutral molecule which undergoes a structural isomerization process. When the desired isomeric structure that correspond to the reactive cationic isomer is reached, the probe laser pulse ionizes the neutral cluster and the chemical reaction is carried out by the positively charged clusters (Fig. 6.8 (c)). The reaction products are then detected by means of mass spectrometry.

The first implementation of the reactive NeNePo spectroscopy was successfully performed in the case of negatively charged silver dimers, in the experiments performed in the group of Prof. L. Wöste.[79] The "classical" NeNePo transient signal of pure $Ag_2$ clusters shows an oscillatory structure with a periodicity of $t = 180\ fs$ which can be attributed to the wave packet oscillations on the electronic ground state of the neutral silver dimer. From investigations of the reactivity of negatively charged silver dimers towards oxygen, it is known that $Ag_2^-$ clusters adsorb one molecule of oxygen and the reaction product $Ag_2O_2^-$ is formed. After the production of the $Ag_2O_2^-$ complex at an ion trap temperature of $T_{octopole} = 100\ K$, the pump and the probe laser beams were directed inside the octopole ion trap. Since the neutral $Ag_2O_2$ complex is not stable, it will rapidly dissociate and the fragment-cation $Ag_2^+$ transient signal was measured as a function of the delay time between the pump and the probe laser pulses. Surprisingly, the recorded reactive NeNePo spectrum of the fragment-cation $Ag_2^+$ shows a different oscillatory structure than the pure $Ag_2^+$ cluster, having a periodicity of approximately $t = 230\ fs$. The frequency shift is due to the presence of the oxygen ligand, which induces a variation of the nuclear dynamics of the silver dimer. Thus, the reactive NeNePo spectroscopy allowed the investigation of the fragmentation dynamics of the reaction product $Ag_2O_2$ in real time.[79]

In the following, the first steps for applying the reactive NeNePo spectroscopy to the study of the fs-dynamics of negatively charged gold cluster-adsorbate complexes will be presented.

### 6.3.1 Photodetachment of $Au_2O_2^-$ and $Au_2CO_3^-$ Cluster-Adsorbate Complexes

As shown in section 5.5, negatively charged gold dimers $Au_2^-$ are able to catalyze the oxidation reaction of carbon monoxide with the $Au_2CO_3^-$ / $Au_2(CO)O_2^-$ complexes as reaction intermediates. The reaction intermediate corresponding to the mass of the $Au_2(CO)O_2^-$ complex presents many structural isomers (structure $A$, $B$, $C$, $D$ and $E$ shown in Fig. 5.25) and only two isomers are involved in the catalytic cycle for the $CO$ oxidation reaction (structure $C$ and $D$). In such a case, the reactive NeNePo spectroscopy is well suited for the identification of different isomers and the investigation of the fs-dynamics of the respective cluster-adsorbate complexes. In this section, the first step of the reactive NeNePo spectroscopy, *i.e.* the photodetachment process will be discussed.

The experimental procedure is the following: the negatively charged $Au_2^-$ clusters are introduced inside the octopole ion trap and exposed to a mixture of reactive gases, $O_2/CO$. During the chemical reaction, the laser is blocked by a mechanical shutter. After a given reaction time $t_{reaction}$, the shutter is opened and the laser beam is directed into the octopole ion trap. The operation of the laser shutter, as well as the entrance and exit electrostatic lenses of the ion trap are computer controlled. The interaction between the negatively charged cluster-adsorbate complexes and the laser beam occurs for a given time $t_{laser}$, after which the laser shutter is closed and the remaining anions are extracted from the octopole ion trap and analyzed with the second quadrupole mass spectrometer.

Fig. 6.9 shows the mass spectrum for the reactivity of $Au_2^-$ clusters towards oxygen and carbon monoxide (grey line) measured for a reaction time of $t_{reaction} = 1000\ ms$ at a temperature of the octopole ion trap of $T_{octopole} = 100\ K$. The peaks corresponding to the $Au_2^-$, $Au_2O_2^-$ and $Au_2(CO)O_2^-$ reaction products can be observed. The photodepletion mass spectrum (black line) was measured after an opening time of the laser shutter of $t_{laser} = 2000\ ms$. Since the repetition rate of the laser system has a value of 1 $kHz$, an opening time of the laser shutter of $t_{laser} = 2000\ ms$ corresponds to 2000 laser pulses which irradiate the reaction educts and products inside the octopole ion trap. The laser beam has a central wavelength of $\lambda = 400\ nm$ and a power of $P_{laser} = 30\ mW$. In the case of the photodepletion mass spectrum depicted

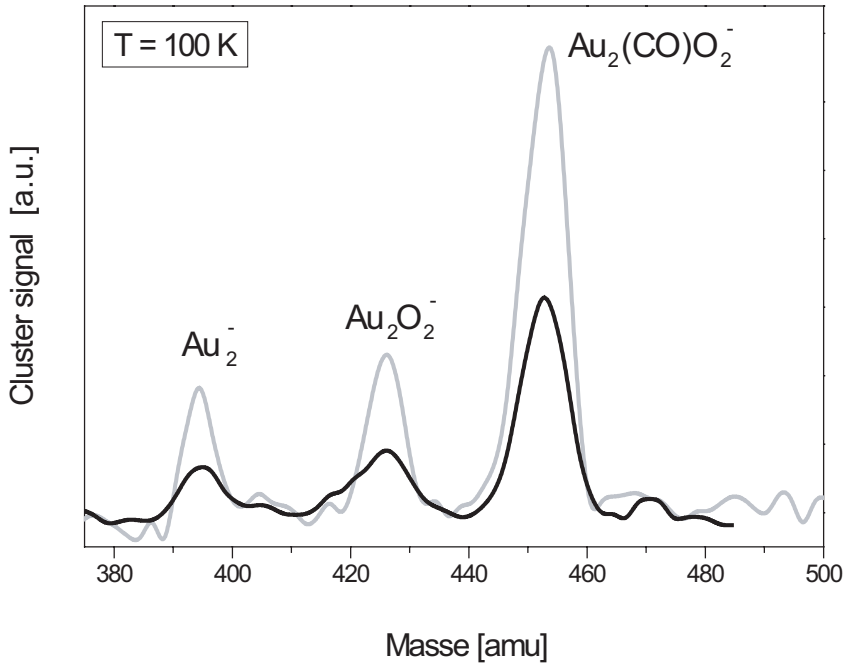


Figure 6.9: Mass spectrum for the reaction of $Au_2^-$ clusters with $O_2$ and $CO$ (grey line). The reaction parameters are: $p_{He} = 0.97\ Pa$, $p_{O_2} = 0.02\ Pa$, $p_{CO} = 0.02\ Pa$, $t_{reaction} = 1000\ ms$, $T_{octopole} = 100\ K$. The photodepletion mass spectrum (black line) is measured after $t_{laser} = 2000\ ms$ at a wavelength of $\lambda = 400\ nm$ and a laser power of $P_{laser} = 30\ mW$.

in Fig. 6.9, the laser beam was focused inside the octopole ion trap by using a lens with a focal distance of $f = 1\ m$.

From Fig. 6.9, it can be seen that the interaction with the laser beam leads to a decrease of the $Au_2^-$, $Au_2O_2^-$ and $Au_2(CO)O_2^-$ signal of about 65 %, 60 % and 55 %, respectively. It is important to note that no product fragmentation is observed as a result of the laser irradiation. This can be seen from the corresponding decrease in the $Au_2^-$ and $Au_2O_2^-$ signals in the mass spectrum shown in Fig. 6.9.

Since the vertical detachment energy of $Au_2^-$ and $Au_2O_2^-$ were experimentally found to be $E_{VDE}(Au_2^-) = 2.01\ eV$[138,158] and $E_{VDE}(Au_2O_2^-) = 3.11\ eV$,[115] respectively and the laser pulse has a central wavelength of $\lambda = 400\ nm$, which corresponds to a photon energy of 3.1 $eV$, a photodetachment process takes place during the interaction with the laser beam, *i.e.* the excess electron from $Au_2^-$ cluster and $Au_2O_2^-$

cluster-adsorbate complex is removed. Hence, the corresponding signal of the $Au_2^-$ and $Au_2O_2^-$ anions is depleted.

In the case of the reaction product corresponding to the mass of $Au_2(CO)O_2^-$ complex, the theoretical calculations predict structural isomers which possess different vertical detachment energies. For the digold carbonate complex $Au_2CO_3^-$ (structure $D$ in Fig. 5.25) a vertical detachment energy of $E_{VDE}(Au_2CO_3^-) = 4.67\ eV$ was calculated, while for the structures $CO - Au_2 - O_2^-$ (structure $A$ in Fig. 5.25) and $Au_2 - CO - O_2^-$ (structure $C$ in Fig. 5.25) a value of $E_{VDE}(CO - Au_2 - O_2^-) = 2.82\ eV$ and $E_{VDE}(Au_2 - CO - O_2^-) = 3.82\ eV$ for the vertical detachment energy was predicted. Moreover, an activation barrier of 0.3 $eV$ was calculated to be involved in the formation of the $Au_2CO_3^-$ reaction product.[57,150] Taking into account the focusing of the laser beam, it could be assumed that, in the mass spectrum presented in Fig. 6.9, one-photon as well as multi-photon absorption are involved in the depletion process. Since the formation of the $Au_2CO_3^-$ complex requires an energetic activation, at an ion trap temperature of $T_{octopole} = 100\ K$ the structure $A$ and $C$ can be observed. For an unambiguous assignment of the $Au_2(CO)O_2^-$ isomeric structures, laser pulse wavelength dependent as well as temperature-dependent photodepletion measurements would be necessary. In conclusion, photodepletion measurements combined with theoretical calculations are able to distinguish between various structural isomers of negatively charged cluster-adsorbate complexes.

The photodetachment process represents the first step of the reactive NeNePo spectroscopy on the $Au_2(CO)O_2^-/Au_2CO_3^-$ cluster-adsorbate complex. Different possible scenarios can be imagined for this system: after the removal of the excess electron, the complex might dissociate and the dynamics of the $Au_2$-fragment could be observed by employing a second time-delayed fs-probe pulse that ionizes the $Au_2$-fragment. In this case, the dissociation process could be monitored in real time. Similar to the reactive NeNePo spectroscopy measurements on $Ag_2O_2^-$ cluster-adsorbate complex, it could be possible to observe a shift in the vibrational frequency of the $Au_2$-fragment compared to pure gold clusters. If the neutral and cationic cluster-adsorbate complex is stable and a geometrical rearrangement takes place, the investigation of the nuclear dynamics of the neutral cluster-adsorbate complex could be carried out by employing the reactive NeNePo spectroscopy.

Theoretical calculations performed in the group of Prof. V. Bonačić-Koutecký pre-

dict a stable structure of the neutral $Au_2(CO)O_2$ and positively charged $Au_2(CO)O_2^+$ species.[178] However, theoretical calculation of the potential energy surfaces of the investigated system as well as calculated values of the vertical detachment energies and ionization potentials are necessary for the implementation of the reactive NeNePo spectroscopy in the case of $Au_2(CO)O_2^-/Au_2CO_3^-$ cluster-adsorbate complex.